

Photochemical & Photobiological Sciences

Accepted Manuscript



This is an *Accepted Manuscript*, which has been through the Royal Society of Chemistry peer review process and has been accepted for publication.

Accepted Manuscripts are published online shortly after acceptance, before technical editing, formatting and proof reading. Using this free service, authors can make their results available to the community, in citable form, before we publish the edited article. We will replace this *Accepted Manuscript* with the edited and formatted *Advance Article* as soon as it is available.

You can find more information about *Accepted Manuscripts* in the [Information for Authors](#).

Please note that technical editing may introduce minor changes to the text and/or graphics, which may alter content. The journal's standard [Terms & Conditions](#) and the [Ethical guidelines](#) still apply. In no event shall the Royal Society of Chemistry be held responsible for any errors or omissions in this *Accepted Manuscript* or any consequences arising from the use of any information it contains.

Cite this: DOI: 10.1039/c0xx00000x

www.rsc.org/xxxxxx

ARTICLE TYPE

Coumarin Containing Star Shaped 4-arm Polyethylene glycol (PEG): Targeted Fluorescent Organic Nanoparticles for efficient Dual treatment of Photodynamic therapy (PDT) and Chemotherapy

Moumita Gangopadhyay,^a Tanya Singh,^b Krishna Kalyani Behara,^a Surendra Karwa,^a S. K. Ghosh,^{*b} and N. D. Pradeep Singh^{*a}

Received (in XXX, XXX) Xth XXXXXXXXX 20XX, Accepted Xth XXXXXXXXX 20XX

DOI: 10.1039/b000000x

Single component fluorescent organic polymeric nanoparticles (NPs) has been synthesized based on a star shaped 4-arm PEG containing coumarin chromophore for concomitant employment of Photodynamic therapy (PDT) and chemotherapy synergistically to wipe out tumour cells with high efficiency. Polymeric NPs are emerging as the most promising nanoparticulates in the area of drug delivery systems due to their ability to overcome the disadvantages like premature and imprecise control over the drug release, lack of loading capacity etc. Among Polymeric NPs, star shaped branched polymers have captured great attention mainly due to their multiple functionalization property. Hence, we, herein, have made use of a multi-arm PEG, functionalized with a targeting unit biotin and a coumarin fluorophore for site-specific and image guided synergic treatment to cancer cells. Anticancer drug chlorambucil is released by coumarin chromophore in a photocontrolled manner. In addition to that, coumarin also generated singlet oxygen upon irradiation with UV/vis light (≥ 365 nm) with a moderate quantum yield of ~ 0.37 . In vitro application of thus prepared organic polymeric nanoparticles (PEG-Bio-Cou-Cbl) in Hela cell line shows reduction of cell viability of upto $\sim 5\%$ in case of combined treatment of PDT and chemotherapy whereas an analogous organic polymeric NPs without the chemotherapeutic drug (PEG-Bio-Cou) results in $\sim 49\%$ cell viability by exhibiting only PDT process.

1. Introduction

Drug Delivery Systems (DDSs) have shown great promise to overcome some inherent problems of commonly available pharmaceuticals e.g. leaching, low solubility in physiological system, undesirable interactions with various physiological environments other than the target site, decomposition etc.^{1,2} Of late, DDSs based on metal nanoparticles (NPs), ceramic NPs, organic NPs, liposomes, polymeric NPs, micelles, Dendrimers etc are being well explored.² Among these, polymeric NPs are fetching utmost attention because of its advantageous properties like enhanced stability of drugs, improved controlled release ability, prolonged blood circulation of the drugs, inhibition of nonspecific interactions of the drugs with the body etc.^{3,4} Poly(ethylene glycol) (PEG) having greatest stealth behaviour⁴ among all polymers, are being widely exploited in therapeutic modalities. PEGs are most promising in their star shaped multi-arm forms than their linear forms. Star shaped polymers are a class of three-dimensional hyperbranched structures where linear arms of same or different molecular weight stem from a single central branch point.⁵ Multiple armed PEG polymers have several advantages in comparison to linear PEG polymers which includes multiple functionality signifying high drug loading efficiency, compact structure i.e. lower static viscosity, greater

hydrodynamic volume and radius of gyration etc.⁶

In the view of conquering the inadequacy of single therapeutic modalities to treat cancer completely, scientists are going after combined treatment of more than one therapeutic method for abolition of tumour cells to a satisfactory level. To date, several combinations of treatments have been tried e.g. "PDT with chemotherapy"⁷⁻⁸, "Photothermal therapy (PTT) and chemotherapy"⁹⁻¹⁴, "PTT with PDT"¹⁵⁻¹⁷. But in all these examples two separate systems were used for the respective treatment modalities. A great number of nano DDSs comprised of gold nanomaterials, graphene oxide (GO) as well as upconversion nanoparticles (UCNPs) have been utilized so far for the aforesaid dual drug administration processes.¹⁸ Recently, we reported such combination of PDT and chemotherapy using semiconducting NPs TiO₂.¹⁹ Nevertheless, all such inorganic NPs bring about potential toxicity due to long time retention inside animal body, hence there is a need to develop organic based single component DDSs for competent combination therapy.

Herein, we report a new single component targeted organic polymeric nano DDS based on star shaped 4-arm PEG decorated with biotin and coumarin chromophore which demonstrates both PDT (Photodynamic Therapy) as well as chemotherapy from a single organic molecule. At the same time, such newly prepared targeted organic polymeric nano DDS can also be handy for

image guided therapy due to inherent fluorescence property of coumarin (**Figure 1**). Although, coumarins have an absorption in UVA range, still they can be explored as a photosensitizer and phototrigger molecule as a proof of concept due to their strong biocompatibility and two-photon absorbing ability. Using coumarin as the organic molecule in our present work renders advantages like coumarin can itself show PDT and simultaneously can release the chemotherapeutic drug chlorambucil upon irradiation of light. Such synergic behaviour of the newly synthesized single component organic polymeric NPs has also been investigated *in vitro* using cancerous Hela Cell line.

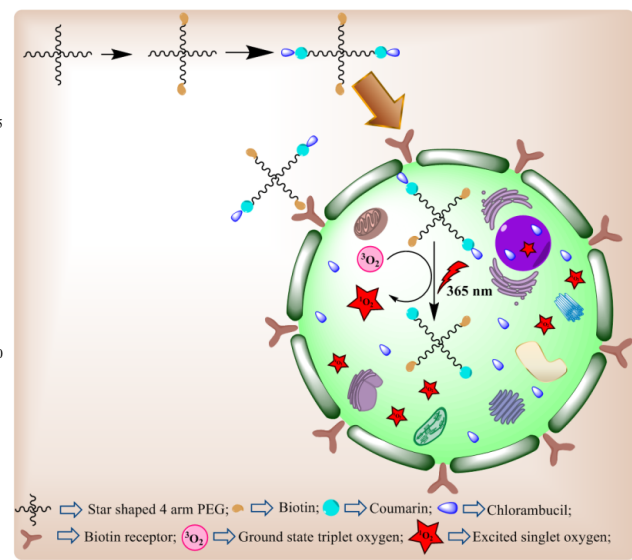


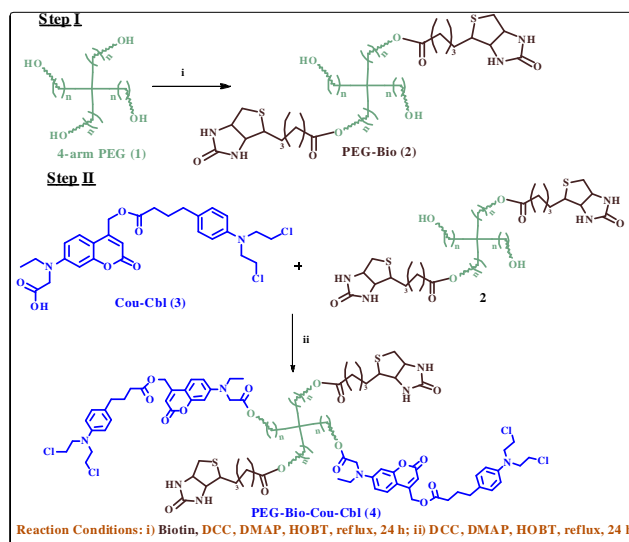
Figure 1 Schematic representation showing synergic effect of PDT and Chemotherapy from biotinylated coumarin polymeric organic NPs based on star shaped 4-arm PEG

2. Result and Discussion:

2.1 Functionalization of 4-arm PEG with biotin and Coumarin-Chlorambucil (Cou-Cbl) conjugate [PEG-Bio-Cou-Cbl] (4):

Polyethylene glycol-biotin-coumarin-chlorambucil conjugate viz. PEG-Bio-Cou-Cbl (**4**) was synthesized in two steps. In first step, the 4-arm PEG i.e. 4-arm Polyethylene glycol (MW= 19,998), (**1**) was decorated with biotin leading to Polyethylene glycol-biotin conjugate i.e. PEG-Bio (**2**) in 87% yield following literature reports²⁰ as shown in **Scheme 1**. Azeotropically dried 4-arm PEG was dissolved in dry DCM and refluxed for 24 h with Biotin (2 eqv) in presence of DCC, HOBT and catalytic amount of DMAP. After 24 h, the desired PEG-Bio (**2**) was recovered by triturating with 2-propanol.

In second step, the PEG-Bio (**2**) was further functionalized with Cou-Cbl (**3**) conjugate using the above described procedure to form PEG-Bio-Cou-Cbl (**4**) in 90% yield. The Cou-Cbl (**3**) conjugate was synthesized following reported procedures²¹⁻²³ (**scheme S1, figure S1-S3**).



Scheme 1 Synthesis of 4-arm PEG functionalized with biotin and Coumarin-Chlorambucil conjugate [PEG-Bio-Cou-Cbl]

2.2 Characterization of PEG-Bio-Cou-Cbl : Absorption, Emission, IR spectra and MALDI-TOF Analysis

Absorption and emission spectra were recorded to prove the formation of PEG-Bio-Cou-Cbl (**Figure 2**). In the absorption spectra PEG-Bio-Cou-Cbl showed two peaks ~250 and ~364 nm due to $\pi-\pi^*$ and $n-\pi^*$ transitions of coumarin moiety respectively. Unmodified PEG in H₂O shows no significant absorbance from 240 to 360 nm and therefore the characteristic absorbance peak of the PEG-Bio-Cou-Cbl at 364 nm is indicative of the attached Cou-Cbl moiety (**Figure 2a**).

A strong increment in fluorescence with a maxima ~480 nm in case of PEG-Bio-Cou-Cbl further indicates the successful covalent attachment of Cou-Cbl with non-fluorescent 4-arm PEG (**Figure 2b**). Thus, from the aforesaid absorption and emission spectral studies, the successful conjugation of Cou-Cbl (**3**) with 4-arm PEG is confirmed.

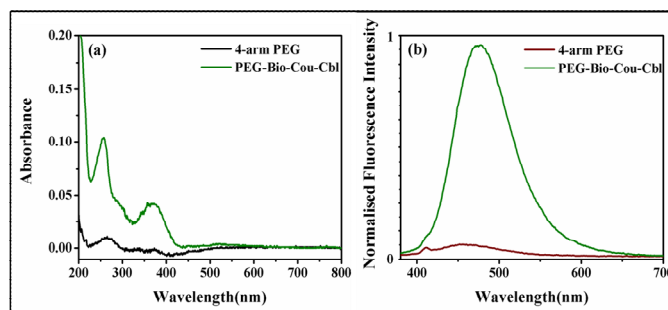


Figure 2 (a) UV/vis and (b) Fluorescence spectra of PEG-Bio-Cou-Cbl

Further the formation of PEG-Bio (**2**) and PEG-Bio-Cou-Cbl (**4**) was analysed with the help of IR spectra. **Figure 3a** represents the IR spectra of free 4-arm PEG. Initially, the attachment of two units of biotin with the two terminal OH groups of 4-arm PEG is supported by appearance of peaks around $\sim 1648\text{ cm}^{-1}$ and $\sim 3449\text{ cm}^{-1}$ (**Figure 3b**),²⁴ which are characteristics for the C=O stretch of newly formed ester linkage between Biotin and 4 arm PEG and stretching frequencies of the remaining terminal O-H groups of 4-

arm PEG respectively. In case of PEG-Bio-Cou-Cbl (**Figure 3c**), appearance of two new C=O stretching frequencies $\sim 1566\text{ cm}^{-1}$ for coumarinyl ester and 1678 cm^{-1} for newly formed ester linkage with PEG-Bio, were indicative of successful conjugation between PEG-Bio (**2**) and Cou-Cbl (**3**).²⁴ Moreover, peaks for remaining terminal O-H groups $\sim 3449\text{ cm}^{-1}$ in PEG-Bio (**Figure 3b**) almost disappeared in the IR spectrum of PEG-Bio-Cou-Cbl (**Figure 3c**), which also suggested the complete functionalization of all four terminal O-H groups of 4-arm PEG.

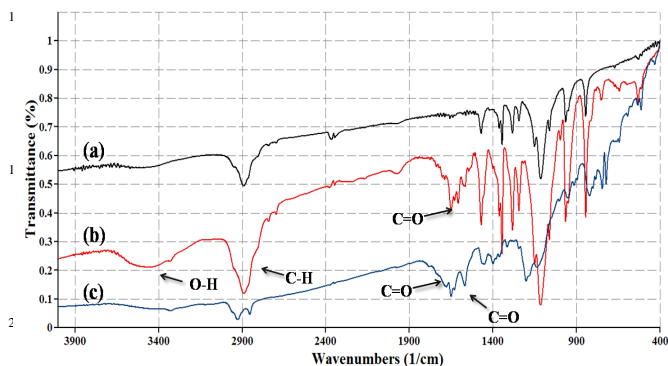


Figure 3 IR overlay spectra of (a) 4-arm PEG, (b) PEG-Bio, (c) PEG-Bio-Cou-Cbl

Thereafter, the two step synthesis of PEG-Bio-Cou-Cbl (**4**) was monitored through MALDI-TOF study.²⁵ For PEG-Bio (**2**), the mass value was obtained around 20451.13 Da (**Figure S4**), which is in accordance with the calculated mass (+ 2 Biotin units- 2 H_2O units) indicating conjugation of 2 units of biotin in two arms of the 4-arm PEG. In the subsequent step, peak $\sim 21575.45\text{ Da}$ was observed for PEG-Bio-Cou-Cbl (**4**) supporting the attachment of total 2 Cou-cbl (**3**) units and 2 Biotin units in the 4 -OH terminals of the star shaped 4-arm PEG. Molecular weight of this newly formed polymer PEG-Bio-Cou-Cbl was also verified by GPC (**Figure S5** (b)).

2.3.1 Synthesis of fluorescent polymeric NPs based on 4-arm PEG-Bio-Cou-Cbl

Further, 4-arm PEG-Bio-Cou-Cbl polymeric NPs were prepared using reprecipitation technique²⁶ and characterized by TEM, DLS and zeta potential measurements

2.3.2 Characterization of PEG-Bio-Cou-Cbl NPs: TEM, DLS and Zeta potential Measurements

The size and shape of the organic polymeric NPs were observed by the TEM study. The representative TEM, DLS and zeta potential studies of the PEG-Bio-Cou-Cbl polymeric NPs are presented in **figure 4a-c**. TEM image (**figure 4a**) shows that the organic polymeric NPs are well separated and globular. The average size of the NPs was found to be $\sim 60\text{ nm}$.

DLS data showed that the PEG-Bio-Cou-Cbl polymeric NPs were of $\sim 68\text{ nm}$ (**Figure 4b**) in size on an average, which is slightly higher compared to the values obtained from TEM analysis.

Further, the zeta potentials values for free PEG and PEG-Bio-Cou-Cbl NPs were recorded. Free PEG showed zeta potential value of -0.057 mV whereas value for PEG-Bio-Cou-Cbl polymeric NPs decreased gradually to 0.0757 mV (**Figure 4c**). Such lowering in the negative value of zeta potential of free 4-

arm PEG also indicates replacement of the terminal OH groups of 4-arm PEG by Biotin and Cou-Cbl (**3**).²⁷ The CMC of PEG-Bio-Cou-Cbl (**4**) NPs was found to be $1.013 \times 10^{-5}\text{ (M)}$ (**Figure S6**).

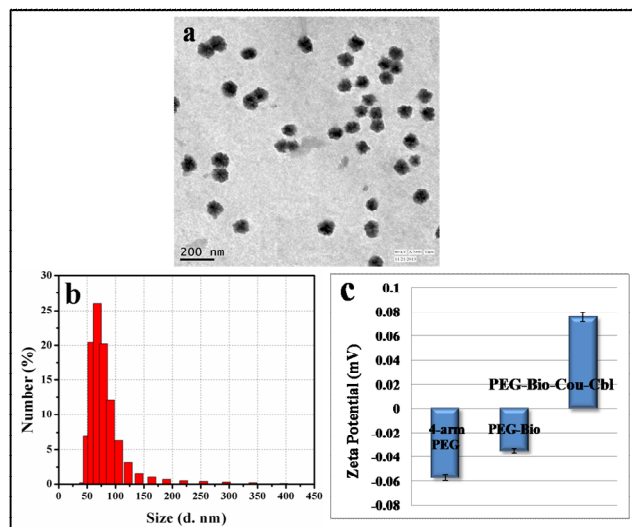


Figure 4 (a) TEM, (b) DLS, (c) Zeta potential studies of PEG-Bio-Cou-Cbl NPs

2.4 Photochemical properties of PEG-Bio-Cou-Cbl NPs

2.4.1 Evidence of PDT activity of PEG-Bio-Cou-Cbl NPs²⁸

After successfully synthesizing and characterizing the newly formed PEG-Bio-Cou-Cbl NPs, we were keen to estimate its photodynamic therapeutic ability. To monitor the efficiency of singlet oxygen generation, we prepared chlorambucil free analogue of PEG-Bio-Cou-Cbl i.e. PEG-Bio-Cou with the intention to eliminate any effect of chlorambucil on the singlet oxygen generation process (See SI, section 5, scheme S2, **Figure S8-S13**). We carried out the well established photodegradation process of 1,3-diphenylisobenzofuran (DPBF) in presence of PEG-Bio-Cou NPs using toluene as solvent to detect its ability of generating singlet oxygen for proficient PDT under the irradiation of $\geq 365\text{ nm}$ light at a fluence rate of 20 mW/cm^2 using 125 W medium pressure Hg vapour lamp. The absorbance of DPBF at 425 nm was found to largely decrease in presence of PEG-Bio-Cou NPs with increasing time, which is a direct evidence of singlet oxygen generation from the said NPs (**Figure 5**). From the slope of the curve, the singlet oxygen quantum yield of PEG-Bio-Cou NPs was calculated as 0.37 (TPP was used as reference with Φ_{Δ} of 0.68) which is slightly higher to the previous report from our group¹⁹ using TiO_2 NPs ($\Phi_{\Delta} = 0.29$) for combination therapy. Further, for coumarin free PEG NPs the singlet oxygen quantum yield was observed as only 0.06. Hence, our aim of replacing toxic inorganic NPs with biocompatible organic DDSs without any loss of therapeutic potential was successful. Further to better mimic physiological environment, we calculated singlet oxygen quantum yield of PEG-Bio-Cou NPs in citrate buffer solution containing 10% acetonitrile (**figure S7**) and the quantum yield was found to be 0.34 (rose bengal was used as reference with Φ_{Δ} of 0.83).

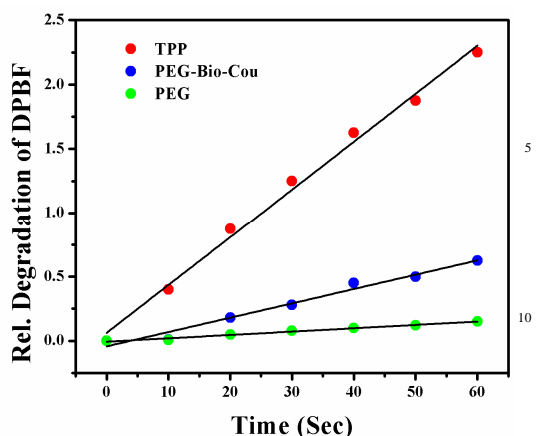


Figure 5 Photodegradation rate of DPBF in the presence of PEG, PEG-Bio-Cou NPs and TPP at 425 nm

2.4.2 Photoinduced anticancer drug release by PEG-Bio-Cou-Cbl NPs²⁹

After successfully addressing the PDT efficacy of PEG-Bio-Cou NPs, we investigated the photoinduced release of anticancer drug chlorambucil from PEG-Bio-Cou-Cbl NPs. To achieve this goal, a aqueous solution of PEG-Bio-Cou-Cbl NPs was irradiated by UV/vis light of wavelength ≥ 365 nm. The photorelease of anticancer drug chlorambucil was monitored using reverse phase HPLC (**Figure S14**). After 60 min of illumination $\sim 80\%$ chlorambucil was effectively released (**Figure 6a**). Thereafter, the control over the phototriggered drug release was also scrutinized by the release of the anticancer drug after periodic exposure to light and dark condition. **Figure 6b** evidently showed that the release of drug took place only in presence of light. The photochemical quantum yield for the release was calculated as

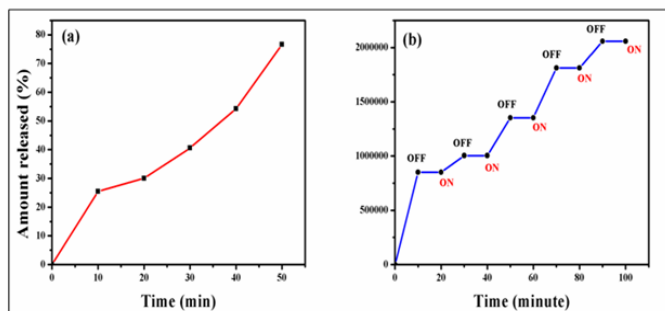


Figure 6 (a) Percentage of chlorambucil released from PEG-Bio-Cou-Cbl; (b) partial progress for the release of chlorambucil under bright and dark conditions. "ON" indicates the beginning of light irradiation; "OFF" indicates the ending of light irradiation

2.5 Photophysical properties of PEG-Bio-Cou-Cbl NPs: Transient absorption and Triplet state lifetime investigations³⁰

The excited state properties of the PEG-Bio-Cou-Cbl NPs were also investigated via nanosecond time-resolved laser flash photolysis for better understanding of its singlet oxygen generation aptitude. Ethanol Solutions of the PEG-Bio-Cou-Cbl NPs in Ar saturated and in O₂ saturated mode were irradiated at 370 nm giving rise to the respective transient spectra (**Figure 7**). Peaks corresponding to triplet-triplet absorption appeared at ~ 460 nm. First-order decay profiles were obtained for both Ar and O₂ saturated solutions. The triplet excited lifetimes were found to be

$\sim 2.743 \mu\text{s}$ for Ar saturated and $\sim 2.003 \mu\text{s}$ for O₂ saturated solution. The quenching of the triplet state lifetime of the PEG-Bio-Cou-Cbl NPs in presence of ground state molecular oxygen ($^3\text{O}_2$) further verified the energy transfer process from the triplet excited state of the NPs to the triplet ground state of O₂ leading to formation of excited singlet oxygen ($^1\text{O}_2$). Higher triplet excited state lifetime of PEG-Bio-Cou-Cbl NPs explains the greater singlet oxygen quantum yield (~ 0.37) value for these organic polymeric NPs compared to inorganic DDS based on TiO₂ NPs as reported previously from our group¹⁹.

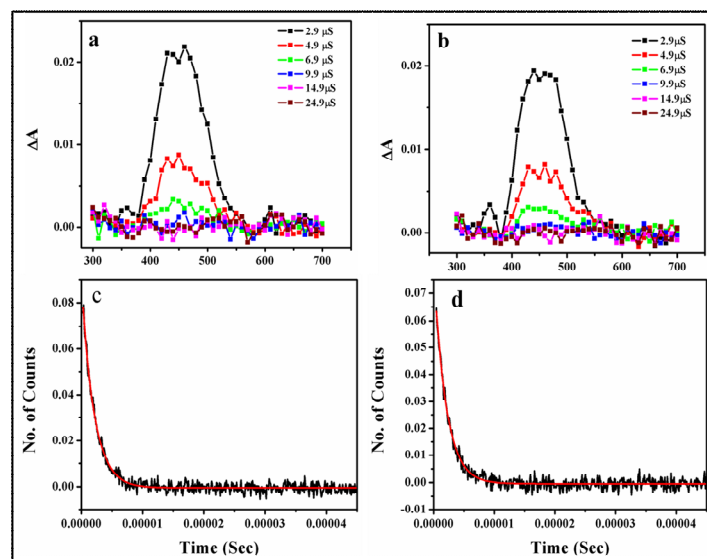


Figure 7 (a-b) Transient absorption spectra (c-d) Decay profile of triplet excited state of PEG-Bio-Cou-Cbl NPs in Ar and O₂ saturated ethanol solution, respectively.

2.6.1 Cellular localization of PEG-Bio-Cou-Cbl NPs

To establish the utilization of PEG-Bio-Cou-Cbl organic polymeric NPs as a handy photoresponsive nano DDSs, cellular internalization efficacy of the NPs was studied on Hela cell line using confocal microscopy.³¹ After incubation of cells with PEG-Bio-Cou-Cbl NPs for different time intervals, blue fluorescence (Excitation and emission maxima 370/461) and accumulation of the NPs was observed in cell cytoplasm. PI staining studies revealed that the NPs were mostly distributed throughout the cytoplasm surrounding the nucleus. In **figure 8 (d1-d2)**, we noticed non-overlapping red emission band at 625 nm for PI and the blue emission band at 461 nm for PEG-Bio-Cou-Cbl NPs indicating the allocation of PEG-Bio-Cou-Cbl NPs mostly in the periphery of nucleus. In a similar way, we also monitored the distribution and accumulation of non-targeted polymeric NPs i.e. non-biotinylated coumarin containing polymeric NPs (PEG-Cou-Cbl NPs) inside the Hela cells. The confocal microscopic study with such non-targeted NPs (**figure S15-S16**) showed PEG-Cou-Cbl NPs internalized into the tumour cells to a lesser extent than the targeted PEG-Bio-Cou-Cbl NPs. To further establish the tumour cell targeting property of the organic polymeric NPs PEG-Bio-Cou-Cbl, we carried out cellular internalization study of PEG-Bio-Cou-Cbl NPs in non-cancerous cell line L929 (**Figure 8(a3)-(d4)**). Comparative cellular internalization studies between Hela cells (**Figure 8(a1)-(b2)**) and L929 cells (**Figure 8(a3)-**

(b4)) indicated that the NPs were selective towards the cancerous HeLa cells, which was due to the presence of biotin moiety in the NPs. The quantification of such selective cellular uptake of PEG-Bio-Cou-Cbl NPs into the HeLa cell was done by measuring the average fluorescence intensity per cell using software of confocal microscopy (figure S17).

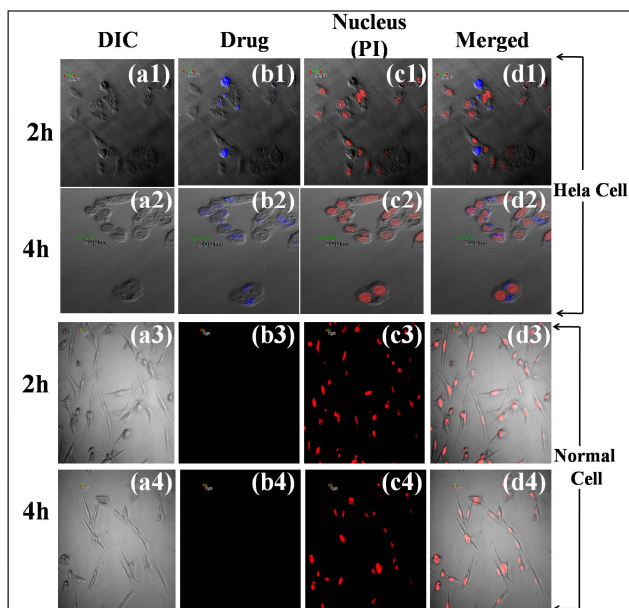


Figure 8 Cellular internalization study of PEG-Bio-Cou-Cbl NPs with PI using confocal microscopy; (a) bright field images, (b-c) fluorescence images (b) in the 625 nm (PI) and (c) 461nm (PEG-Bio-Cou-Cbl NPs) emission channels and (d) overlays of the bright-field images and the fluorescence images in (1-2) HeLa cell line and (3-4) Normal L929 cell line.

2.6.2 *In vitro* Cell cytotoxicity study of PEG-Bio-Cou-Cbl NPs before and after photolysis

After the photochemical and photophysical studies, we were interested to observe the *in vitro* toxicity of the PEG-Bio-Cou-Cbl NPs against cancer cells. We evaluated cell viability using MTT assay in HeLa cancer cell line.³² Cells were incubated with PBS, PEG, free chlorambucil (Cbl), PEG-Bio-Cou-Cbl, PEG-Bio-Cou separately for 4h at different concentrations viz. 50, 100, 150 and 250 $\mu\text{g/mL}$. After incubation, the cells were illuminated with UV/vis light (≥ 365 nm) and further incubated for 24 h. As per our expectation, we observed enhanced cell cytotoxicity in case of PEG-Bio-Cou-Cbl NPs compared to both PEG-Bio-Cou NPs and free Chlorambucil. From **figure 9**, it is clearly noted that after 20 min of irradiation there is a large increase of cell destruction for PEG-Bio-Cou-Cbl NPs as indicated by $\sim 34\%$ cell viability compared to $\sim 69\%$ cell viability for PEG-Bio-Cou NPs. Again, after 60 min of irradiation, only $\sim 5\%$ of the cancer cells survived in case of PEG-Bio-Cou-Cbl NPs whereas $\sim 49\%$ of cell viability was noted for PEG-Bio-Cou NPs. This larger tumor cell destruction for PEG-Bio-Cou-Cbl NPs can be attributed to its combined PDT and chemotherapeutic effect. On the other hand, cell viability was found to be largely unaffected by free 4-arm PEG, indicating the cytotoxicity was likely caused by the dual treatment modalities exhibited by the single Cou-Cbl moiety. Advantage of single component organic DDSs over the semiconducting inorganic analogues based on TiO_2 , as reported

earlier from our group¹⁹, was evident in the percentage of cell viability by PEG-Bio-Cou-Cbl NPs ($\sim 5\%$) which is much lower than our previous report indicating better accumulation of the present single component organic DDSs inside the tumour cell than in normal cells.

The *in vitro* anticancer drug release was also measured in terms of UV spectroscopy using dialysis process (supporting information section 8, figure S18).

The cytotoxic assay of PEG-Bio-Cou, PEG-Bio-Cou-Cbl NPs and free 4-arm PEG were also performed on HeLa cells without irradiation. We observed no significant cell destruction either for PEG-Bio-Cou-Cbl or PEG-Bio-Cou.

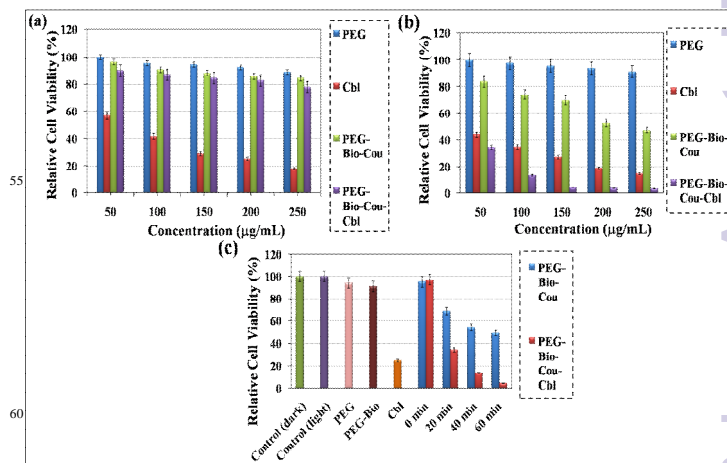


Figure 9 Comparative Cell viability study of PEG-Bio-Cou and PEG-Bio-Cou-Cbl NPs on HeLa cells (a) before illumination, (b) after illuminating 60 min with UV/vis light (≥ 365 nm) at a fluence rate of 20 mW/cm^2 and (c) decrease of cell viability for PEG-Bio-Cou and PEG-Bio-Cou-Cbl NPs depending on irradiation time. Concentration of free Chlorambucil used 250 $\mu\text{g/mL}$. Values are presented as means \pm standard deviations of three different observations

3. Experimental Section

3.1 Synthesis of PEG-Bio-Cou-Cbl (4)

PEG-Bio-Cou-Cbl (4) was prepared following the stepwise pathway.

Step I : Attachment of 4-arm PEG with biotin (PEG-Bio) (2)²⁰

Biotin was successfully attached with star shaped 4-arm PEG following the literature procedure²⁰ in 87 % yield as shown in **Scheme 1**. 4-arm PEG (0.500 g, ~ 0.025 mmol) (Creative PEG works) was azeotropically dried in vacuo with CHCl_3 and was redissolved in CH_2Cl_2 (10 mL). To this clear solution was added biotin (0.012 g, 0.05 mmol), N,N-dicyclohexylcarbodiimide (DCC) (0.043 g, 0.210 mmol in 10 mL of CH_2Cl_2), 1-hydroxybenzotriazole (HOBT) (0.017 g, 0.126 mmol) and catalytic amount of N,N-dimethylaminopyridine (DMAP) and the mixture was allowed to reflux under nitrogen for 24 h (**scheme 1**). After 24 h, the reaction mixture was evaporated in vacuo and the residual syrup was dissolved in ~ 1 mL toluene and filtered. Toluene was removed in vacuo at 45 $^\circ\text{C}$. To the residue 0.25 mL of CH_2Cl_2 was added and triturated with 1.5 mL 2-propanol. The pure water-soluble product was collected in 87 % yield by vacuum filtration and dried overnight. It was further characterized

by UV/vis, fluorescence, IR spectra and MALDI-TOF analysis.

Step II : Attachment of PEG-Bio (2) with Cou-cbl (PEG-Bio-Cou-Cbl) (4)²⁰

Cou-Cbl (3) was successfully attached with PEG-Bio following the previously mentioned literature procedure in 90 % yield as shown in **Scheme 1**. To a CH₂Cl₂ solution of PEG-Bio (0.100 g, 0.005 mmol), Cou-Cbl (3) (0.016 g, 0.028 mmol, 5 eqv), catalytic amount of DMAP, HOBT (0.004 g, 0.025 mmol) and DCC (0.008 g, 0.042 mmol in about 10 mL of CH₂Cl₂) was added and the mixture was refluxed for 24 h under nitrogen atmosphere. After 24 h, the reaction mixture was evaporated in vacuo and the residual syrup was dissolved in ~1 mL toluene and filtered. Toluene was removed in vacuo at 45 °C. To the residue 0.25 mL of CH₂Cl₂ was added and triturated with 1.5 mL 2-propanol. The pure water-soluble product (0.088 g) was collected in 90 % yield by vacuum filtration and dried overnight. It was characterised by UV/vis, fluorescence, IR spectra and MALDI-TOF analysis.

Synthesis of fluorescent polymeric NPs based on 4-arm PEG-Bio-Cou-Cbl polymer

Reprecipitation technique was followed to synthesize 4-arm PEG-Bio-Cou-Cbl polymeric NPs.²⁶ To a vial containing 20 mL acetone, 10 µL of 3 mM aqueous solution of 4 arm PEG-Bio-Cou-Cbl NPs was slowly added at room temperature under controlled stirring. The size and shape of the 4-arm PEG-Bio-Cou-Cbl NPs was verified by TEM, DLS and zeta potential measurements.

3.2 Photochemical properties of PEG-Bio-Cou-Cbl NPs

3.2.1 Evidence for PDT activity of PEG-Bio-Cou-Cbl NPs²⁸

To study the PDT activity of PEG-Bio-Cou-Cbl NPs, we prepared chlorambucil free NPs PEG-Bio-Cou to eliminate the influence of anticancer drug chlorambucil. In order to confirm the generation of singlet oxygen by PEG-Bio-Cou NPs, we recorded the photodegradation rate of 1,3-diphenylisobenzofuran (DPBF, Aldrich) in presence of the NPs. The singlet oxygen quantum yield (Φ_{Δ}) was determined using Tetraphenylporphyrin (TPP) as the reference having a singlet oxygen quantum yield of 0.68 in toluene.

3.2.2 Evidence for Photoinduced Anticancer Drug release from PEG-Bio-Cou-Cbl NPs²⁹

To monitor the controlled release of anticancer drug chlorambucil from PEG-Bio-Cou-Cbl particles, 5 mL aqueous solution of 30 mg NPs exposed to visible light of wavelength ≥ 365 nm (125 W medium pressure Hg vapour lamp) using 1 M CuSO₄ solution in Millipore water as filter under N₂ atmosphere for 60 min. A 100 µL aliquot of the solution was collected after each 10 min. The collected solutions were then passed through reversed-phase HPLC using 95 : 5 trifluoro acetic acid (TFA) : H₂O solution and 96 : 4 TFA in acetonitrile as mobile phase. Flow rate was maintained at 1 mL/min.

3.3 Photophysical properties of PEG-Bio-Cou-Cbl NPs

Triplet State lifetime measurement³⁰

To assess the characteristics of transient species formed from PEG-Bio-Cou-Cbl NPs. Laser flash photolysis experiment was carried out using a nanosecond flash photolysis set-up (Applied Photophysics). Instrumental details and experimental procedure is explained in supporting information (section 4.1. (ii)).

3.4 Cell imaging and Nuclear localization study of PEG-Bio-Cou-Cbl NPs

To study the cellular uptake of PEG-Bio-Cou-Cbl by cancerous HeLa cell line, 5x10⁴ cells / well were seeded in 24 well plate and was allowed to adhere for 4-8 hrs at 37 °C and 5 % CO₂. The cells were incubated with PEG-Bio-Cou-Cbl NPs for different time intervals in presence of 5 % CO₂. Thereafter, the cells were fixed with 70 % alcohol for 2 hrs at 4 °C followed by RNase A treatment in 2X SSC buffer at 37 °C for 30 min. Finally, nucleus was stained with propidium iodide (2 µg/mL) and visualized by Olympus FV1000 confocal microscope.³¹ To study the cancer cell specificity of the drug, the entire experiment was performed on a non cancerous cell line, L929 as a control.

3.5 In vitro Cell cytotoxicity studies of PEG-Bio-Cou-Cbl NPs in HeLa cells

HeLa cells lines were purchased from National Centre for Cell Science, Pune, India and were maintained in Dulbecco's Modified Eagle's medium (DMEM) supplemented with 10 % fetal bovine serum. Cell culture media and all the other materials required for culturing were obtained from Gibco, USA. Cytotoxicity of PEG-Bio-Cou-Cbl NPs under dark as well as upon exposure to light on HeLa cells was determined by conventional MTT assay.³² HeLa cells were trypsinized and counted using hemocytometer and then seeded in 96-well micro plate at 5x10⁴ cells/mL in DMEM (Dulbecco's modified Eagle medium) complete medium. The cells were incubated at 37 °C in 5 % CO₂ for 24 hrs to allow adherence. The medium was replaced with fresh DMEM incomplete medium containing various concentrations of PEG, chlorambucil (Cbl), PEG-Bio-Cou-Cbl, PEG-Bio-Cou viz. 50, 100, 150 and 250 µg/mL for 4 hrs. After incubation, the cells were illuminated with UV/vis light of wavelength ≥ 365 nm and further incubated for 24 hrs. Cells were then washed with 1XPBS and 100 µL of MTT solution (1 mg/mL) was added to each well. After 3 hrs of incubation, MTT solution was removed and replaced with 200 µL of DMSO. Absorbance was read at 570 nM using microplate reader (Thermo Scientific Multiskan Spectrum, USA). Each sample was assayed in triplicate, and control samples include cells with DMSO.

To establish the synergic effect of PDT and chemotherapy of PEG-Bio-Cou-Cbl NPs *in vitro*, we compared the MTT assay results obtained separately with PEG-Bio-Cou and PEG-Bio-Cou-Cbl NPs upon irradiation of light for different time intervals as described above and found enhanced cytotoxicity for the later particles after same time of irradiation.

4. Conclusion

In conclusion, we have synthesized a new organic polymeric NP based on 4-arm PEG to ensure higher density of functional groups in a small volume compared to their linear analogues. For more specific treatments towards tumour tissues, biotin was covalently attached to the 4-arm PEG as the targeting pendant. Thus prepared globular PEG-Bio-Cou-Cbl NPs with ~60 nm size contained coumarin fluorophore which rendered synergistic treatment to HeLa cell line via concomitant occurrence of PDT and chemotherapy. PEG-Bio-Cou-Cbl NPs showed a moderate singlet oxygen quantum yield as 0.37 at the same time it released almost 80% of anticancer drug chlorambucil upon exposure to UV/vis light of ≥ 365 nm. In vitro application of PEG-Bio-Cou-Cbl NPs in cancerous HeLa cell line suggested greater extent of

cell damage in case of combined effect of PDT and chemotherapy compared to only PDT. Biotin conjugation in PEG-Bio-Cou-Cbl NPs ensured better accumulation of the NPs in Hela cell lines than in non cancerous L929 cells. Thus, for the first time we synthesized an efficient single component targeted photoresponsive organic polymeric NPs based on 4-arm PEG for competent combination therapy of cancer treatment.

Acknowledgement

We thank DST-SERB for sponsorship and DST FIST for 400 MHz NMR. Authors sincerely acknowledge Professor Samita Basu, Chemical Science Division, Saha Institute of Nuclear Physics, Kolkata for triplet state lifetime measurements. Moumita is thankful to IIT Kharagpur for fellowship.

Notes and references

^aDepartment of Chemistry, Indian Institute of Technology, Kharagpur 721302, West Bengal, India
E-mail: ndpradeep@chem.iitkgp.ernet.in

^bDepartment of Biotechnology, Indian Institute of Technology, Kharagpur 721302, West Bengal, India, E-mail: sudip@hijli.iitkgp.ernet.in

[†]Electronic Supplementary Information (ESI) available: Experimental procedures, characterization data like ¹H NMR, ¹³C NMR, TGA, MALDI-TOF, GPC, quantum yield calculation and CMC calculation are included in the supporting information. See DOI: 10.1039/b000000x/

- G. Tiwari, R. Tiwari, B. Sriwastawa, L. Bhati, S. Pandey, P. Pandey, K. S. Bannerjee, Drug delivery systems: An updated review, *Int. J. Pharm. Investig.*, 2012, **1**, 2-11.
- A. Jana, K. T. Nguyen, X. Li, P. Zhu, N. S. Tan, H. A. Gren, Y. Zhao, Perylene-derived single-component organic nanoparticles with tunable emission: Efficient anticancer drug carriers with real-time monitoring of drug release, *ACS Nano*, 2014, **8**, 5939-5952.
- K. S. Soppimath, T. M. Aminabhavia, A. R. Kulkarni, W. E. Rudzinski, Biodegradable polymeric nanoparticles as drug delivery devices, *J. Control. Release*, 2001, **70**, 1-20.
- K. Knop, R. Hoogenboom, D. Fischer, U. S. Schubert, Poly(ethylene glycol) in drug delivery: Pros and cons as well as potential alternatives, *Angew. Chem. Int. Ed.*, 2010, **49**, 6288-6308.
- N. A. Peppas, K. B. Keys, M. Torres-Lugo, A. M. Lowman, Poly(ethylene glycol)-containing hydrogels in drug delivery, *J. Control. Release*, 1999, **62**, 81-87.
- N. H. Aloorkar, A. S. Kulkarni, R. A. Patil, D. J. Ingale, Star polymers: An overview, *Int. J. Pharm. Sci. Nanotech.*, 2012, **5**, 1675-1684.
- J. G. Shiah, Y. Sun, P. Kopec̣ková, C. Peterson, R. Straight, J. Kopec̣ek, Combination chemotherapy and photodynamic therapy of targetable *N*-(2-hydroxypropyl)methacrylamide copolymer-doxorubicin/mesochlorin e₆-OV-TL 16 antibody immunconjugates, *J. Control. Release*, 2001, **74**, 249-253.
- M. Y. Nahabedian, R. A. Cohen, M. F. Contino, T. M. Terem, W. H. Wright, M. W. Berns, A. G. Wile, Combination cytotoxic chemotherapy with Cisplatin or Doxorubicin and photodynamic therapy in murine tumors, *J. Natl. Cancer Inst.*, 1988, **80**, 739-743.
- W. Zhang, Z. Guo, D. Huang, Z. Liu, X. Guo, H. Zhong, Synergistic effect of chemo-photothermal therapy using PEGylated graphene oxide, *Biomaterials*, 2011, **32**, 8555-8561.
- H. Liu, D. Chen, L. Li, T. Liu, L. Tan, X. Wu, F. Tang, Multifunctional gold nanoshells on silica nanorattles: A platform for the combination of photothermal therapy and chemotherapy with low systemic toxicity, *Angew. Chem. Int. Ed.*, 2011, **50**, 891-895.
- X. Ma, H. Tao, K. Yang, L. Feng, L. Cheng, X. Shi, Y. Li, L. Guo, Z. Liu, A functionalized graphene oxide-iron oxide nanocomposite for magnetically targeted drug delivery, photothermal therapy, and magnetic resonance imaging, *Nano Res.*, 2012, **5**, 199-212.
- C. Wang, H. Xu, C. Liang, Y. Liu, Z. Li, G. Yang, L. Cheng, Y. Li, Z. Liu, Iron Oxide @ Polypyrrole nanoparticles as a multifunctional drug carrier for remotely controlled cancer therapy with synergistic antitumor effect, *ACS Nano*, 2013, **7**, 6782-6795.
- G. Song, Q. Wang, Y. Wang, G. Lv, C. Li, R. Zou, Z. Chen, Z. Qin, K. Huo, R. Hu, A low-toxic multifunctional nanoplatfrom based on Cu₉S₅@mSiO₂ core-shell nanocomposites : Combining photothermal- and chemotherapies with infrared thermal imaging for cancer treatment, *Adv. Funct. Mater.*, 2013, **23**, 4281-4292.
- M. heng, C. Yue, Y. Ma, P. Gong, P. Zhao, C. Zheng, Z. Sheng, P. Zhang, Z. Wang, L. Cai, Single-step assembly of DOX/ICG loaded lipid-polymer nanoparticles for highly effective chemo-photothermal combination therapy, *ACS Nano*, 2013, **7**, 2056-5067.
- J. Lin, S. Wang, P. Huang, Z. Wang, S. Chen, G. Niu, W. Li, J. He, D. Cui, G. Lu, Photosensitizer-loaded gold vesicles with strong plasmonic coupling effect for imaging-guided photothermal/photodynamic therapy, *ACS Nano*, 2013, **7**, 5320-5329.
- B. Jang, J. Y. Park, C. H. Tung, I. H. Kim, Y. Choi, Gold nanorod-photosensitizer complex for near-infrared fluorescence imaging and photodynamic/photothermal therapy in vivo., *ACS Nano*, 2011, **5**, 1086-1094.
- J. Y. Kim, W. I. Choi, M. Kim, G. Tae, Tumor-targeting nanogel that can function independently for both photodynamic and photothermal therapy and its synergy from the procedure of PDT followed by PTT, *J. Control. Release*, 2013, **171**, 113-121.
- H. Gong, Z. Dong, Y. Liu, S. Yin, L. Cheng, W. Xi, J. Xiang, K. Liu, Y. Li, Z. Liu, Engineering of multifunctional nanomicelles for combined photothermal and photodynamic therapy under the guidance of multimodal imaging. *Adv. Funct. Mater.*, 2014, **24**, 6492-6502.
- M. Gangopadhyay, S. K. Mukhopadhyay, S. Karthik, S. Barman, N. D. P. Singh, Targeted photoresponsive TiO₂-coumarin nanoconjugate for efficient combination therapy in MDA-MB-231 breast cancer cells: synergic effect of photodynamic therapy (PDT) and anticancer drug chlorambucil, *Med. Chem. Comm.*, 2015, DOI: 10.1039/C4MD00481G.
- M. D. Bentley, X. Zhao, J. L. Clark, Water-soluble polymer conjugates of Artenilic acid, US006461603B2.
- Q. Lin, Q. Huang, C. Li, C. Bao, Z. Liu, F. Li, L. Zhu, Anticancer drug release from a mesoporous silica based nanophotocage regulated by either a one- or two-photon process, *J. Am. Chem. Soc.*, 2010, **132**, 10645-10647.
- V. Hagen, B. Dekowski, V. Nache, R. Schmidt, D. Geißler, D. Lorenz, J. Eichhorst, S. Keller, H. Kaneko, K. Benndorf, B. Wiesner, Coumarinylmethyl esters for ultrafast release of high concentrations of cyclic nucleotides upon one- and two-photon photolysis, *Angew. Chem. Int. Ed.*, 2005, **44**, 7887-7891.
- V. Hagen, B. Dekowski, N. Kotzur, R. Lechler, B. Wiesner, B. Briand, M. Beyermann, {7-[Bis(carboxymethyl)amino]coumarin-4-yl}methoxycarbonyl derivatives for photorelease of carboxylic acids, alcohols/phenols, thioalcohols/thiophenols, and amines, *Chem. Eur. J.*, 2008, **14**, 1621-1627.
- S. Y. Kim, S. H. Cho, Y. M. Lee, Biotin-conjugated block copolymeric nanoparticles as tumor-targeted drug delivery systems, *Macromol. Res.*, 2007, **15**, 646-655.
- R. N. Jagtap, A. H. Ambre, Overview literature on matrix assisted laser desorption ionization mass spectroscopy

(MALDI MS): basics and its applications in characterizing polymeric materials, *Bull. Mater. Sci.*, 2005, **28**, 515-528.

26. K. Baba, H. Kasai, A. Masuhara, H. Oikawa, H. Nakanishi, Organic Solvent-Free Fluorescence confocal imaging of living cells using pure nanocrystal forms of fluorescent dyes, *Jpn. J. Appl. Phys.*, 2009, **48**, 117002.
27. C. S. Lee, W. Park, Y. U. Jo, K. Na, A charge-switchable, four-armed polymeric photosensitizer for photodynamic cancer therapy, *Chem. Commun.*, 2014, **50**, 4354-4357.
28. Q. Zou, I. Zou, Y. Fang, Y. Zhao, H. Zhao, Y. Wang, Y. Gu, F. Wu, Synthesis and in vitro photocytotoxicity of coumarin derivatives for one- and two-photon excited photodynamic therapy, *J. Med. Chem.*, 2013, **56**, 5288-5294.
29. A. Jana, S. Atta, S. K. Sarkar, N. D. P. Singh, 1-Acetylpyrene with dual functions as an environment-sensitive fluorophore and fluorescent photoremovable protecting group, *Tetrahedron*, 2010, **52**, 9798-9807.
30. M. K. Sarangi, Basu, S. Photophysical behavior of acridine with amines within the micellar microenvironment of SDS: a time-resolved fluorescence and laser flash photolysis study, *Phys. Chem. Chem. Phys.*, 2011, **13**, 16821-16830.
31. T. Suzuki, K. Fujikura, T. Higashiyama, K. Takata, DNA staining for fluorescence and laser confocal microscopy, *J. Histochem. Cytochem.*, 1997, **45**, 49-53.
32. S. Karthik, N. Puvvada, K. B. N. Prashanth, S. Rajput, A. Pathak, M. Mandal, N. D. P. Singh, Photoresponsive coumarin-tethered multifunctional magnetic nanoparticles for release of anticancer drug, *ACS Appl. Mater. Interfaces*, 2013, **5**, 5232-5238.